FTD-ID(RS)T-1364-87

FOREIGN TECHNOLOGY DIVISION

EXPERIMENT INVESTIGATION ON LONGITUDINAL CHARACTERISTICS OF THE FORWARD SWEPT WING

by

Guo Yaobin, Wang Xuejian, Zhang Binjiang

Approved for public release;
Distribution unlimited.

HUMAN TRANSLATION

FTD-ID(RS)T-1364-87 10 March 1988

MICROFICHE NR: FTD-88-C-000252

EXPERIMENT INVESTIGATION ON LONGITUDINAL CHARACTERISTICS OF THE FORWARD SWEPT WING

By: Guo Yaobin, Wang Xuejian, Zhang Binjiang

English pages: 25

Source: Hangkong Xuebao, Vol. 8, Nr. 6, June 1987, pp. 227-238

Country of origin: China
Translated by: FLS, Inc.
F33657-85-D-2079
Requester: FTD/TQTA

PREPARED BY:

TRANSLATION DIVISION
FOREIGN TECHNOLOGY DIVISION
WPAFB, OHIO.

GRAPHICS DISCLAIMER

All figures, graphics, tables, equations, etc. merged into this translation were extracted from the best quality copy available.

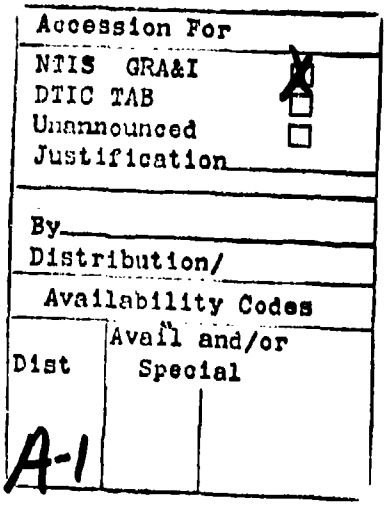

EXPERIMENT INVESTIGATION ON LONGITUDINAL CHARACTERISTICS OF THE FORWARD SWEPT WING

by Guo Yaobin, Wang Xuejian and Zhang Binjiang
(Harbin Aerodynamics Research Institute)

Submitted November 2, 1985

Abstract

Based on testing results of aerodynamic forces and pressures from a wind tunnel, the longitudinal aerodynamics characteristics of a forward swept wing are discussed in this paper. The results are also compared with the data of an associated aft swept wing. Measures of improving the inboard flowfield of a forward swept wing are also investigated, and the results are discussed. Under a low speed situation, an appropriate sweptback of the root section can improve the flow characteristics at that place for a forward swept wing, consequently obtaining higher aerodynamic performances. In addition, if canards are also installed which can further improved the inboard flowfield and obtains a higher lift-drag ratio. For instance, when C_y=0.5, the lift-drag ratio of the swept forward wing which has canards and an appropriate sweptback at its root section (fairing) is 24% higher than that of the strake aft swept wing with canard configuration (both configurations have the same lifting area).

In a transonic regime, the forward swept wing possesses less zero-lift drag and lift induced drag than the aft swept wing. When Ma=1.1, α= 6°, the lift induced drag of the forward swept wing is 12.5% less than that of aft swept wing. The measures of improving the inboard flowfield in a low speed situation can still be applied at this regime. The forward swept wing with an appropriate aft swept inboard (fairing) accompanied by canards can also provide more improvement to the high speed characteristics.

I. Preface

As early as the mid 40's, an airplane with 15° forward swept wings had been made (JU-287). However, the aeroelastic divergence problem stopped its further development. Until the mid 70's, technology breakthrough in the areas of both composite material and auto-control systems provided the means of solving the aeroelastic divergence problem, thus the forward swept wing concept could be widely applied. Therefore, its aerodynamic characteristics necessitates for further studies.

In order to understand the basic aerodynamic characteristics of a forward swept wing, low speed experiments for both forward and aft swept flat plate wings were conducted; flow visualizations were also taken. We observed that the flow separation occurs frequently on the forward swept wing [2]. Therefore, in the following studies, forward and aft swept wings which both have the same absolute swept angles at their 1/4 cord line are used, and the study focuses on the performance upgrade for a forward swept wing configuration by improving its inboard flowfield.

In order to examine aerodynamic interference occurring between a canard and the main wing in the coupled confutation, a dual-balance synchronized measuring technique is adopted for both low and high flow speed experiments.

All coefficients in this paper are presented by taking the basic wing area as a reference.

II. Model and Experiment Equipment

1. Model

A model sketch is shown in Fig. 1. Wing parameters are: λ= 3.2, η= 5.08, χ_0= 40° for aft swept wing and χ_0= -22°46' for forward swept wing; $|\chi_{\frac{1}{4}}|$= 32°11' for both wing configurations. Leading edge flaps and stakes are installed on the wings; a fairing can also be added at the root section of the forward swept wing.

The fuselage of the model has two sections, and they are connected by a strain balance. The front section can have canards installed. This arrangement can allow us to measure aerodynamic forces between the front section of the fuselage and the canards while a main balance measures aerodynamic forces for the entire model.

The high speed model is similar to the low speed one; the parameters of model attachments are given in Table 1. The cross-section at the location of pressure measurement is also shown in Fig. 1.

The airfoil used in experiments is NACA65 $_{A}$-0045. The longitudinal cross-section of the strake is wedge-shaped.

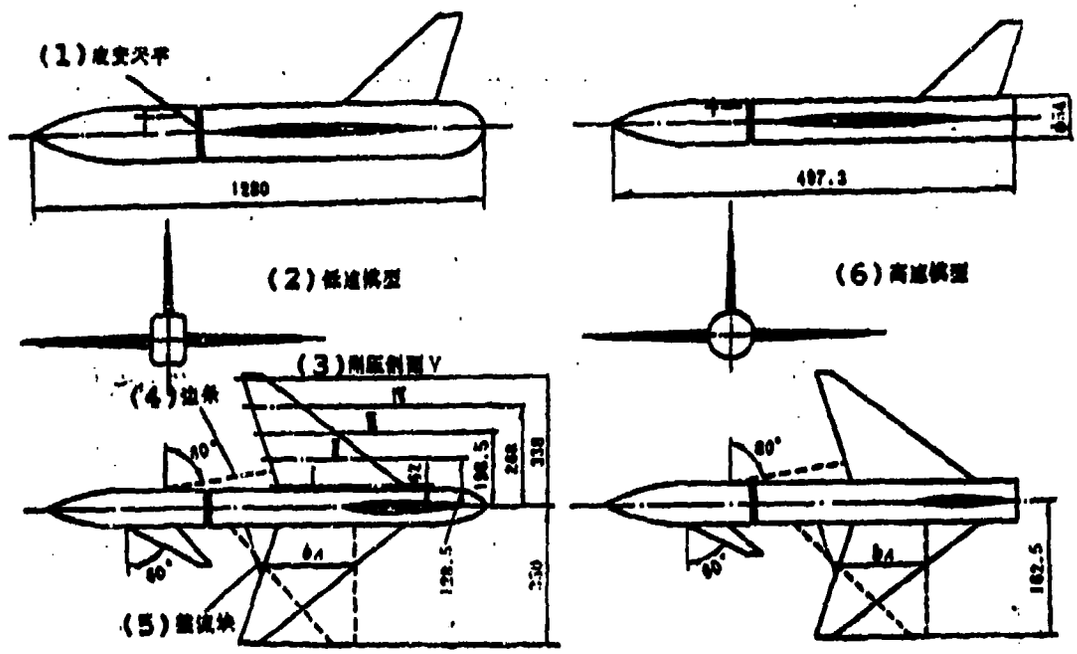

Fig. 1 Sketch of model
Key: (1) Strain balance; (2) Low speed model; (3) Cross-section of pressure measurement location; (4) Strake; (5) Fairing; (6) High speed model.

Table 1 Geometric parameters of model attachments

(1) 模 型	X_0	X_1 对 6	X_1	η	λ	$S(m^2)$
(2) 后掠翼	40°	32°11′	0°	5.08	3.2	0.033
(3) 前掠翼	−32°46′	−32°11′	−51°31′	5.08	3.2	0.033
(4) 大前缘掠角	−39°44′	−43°10′	−51°31′	3.04	3.2	0.033
(5) 小前缘掠角	−8°55′	−33°22′	−51°31′	15.8	3.2	0.033
(6) 大后缘掠角	−32°46′		−58°11′	43	3.2	0.033
(7) 小后缘掠角	−32°46′	′	−40°15′	3.04	3.2	0.033

Key: (1) Model; (2) aft swept wing; (3) forward swept wing; (4) Swept angle of large leading edge; (5) Swept angle of small leading edge; (6) Swept angle of large training edge; (7) Swept angle of small training edge.

2. Experiment Equipment

Low speed experiments are conducted in an open type, circular flow wind tunnel whose test section is 1.5m in diameter, wind speed 30 m/s, experiment Reynold's number Re = 0.51 x 10^6 and whose the characteristic length is based on the average aerodynamic chord.

The test section dimension of the transonic wind tunnel is 0.52x0.64 m. On the four sides of the tunnel wall, there are plates with throttle controlled oblique holes and single point supported semi-flexible nozzles. Experiment Mach number, Ma is in the range of 0.4 and 1.5, the Reynold's number, Re = 0.96 ~ 1.74x10^6 whose characteristic length is based on the average aerodynamic chord.

For the low speed experiment, the aerodynamic forces of the entire model are measured by using a platform type mechanical balance while the loading on the canards is measured by a strain balance. For the high speed experiment, two strain balances are used to measure the aerodynamic forces of the entire model and the canards, respectively. An additional, small loading strain balance is also used to check the aerodynamic measurements for the entire model in the case of a small angle of attack ($\alpha \leq 4°$).

Pressure measurements are conducted by using sensors and scan valves. Measurements can be recorded and processed automatically through the wind tunnel checking system.

III. Low Speed Aerodynamic Characteristics of a Forward Swept Wing

1. Aerodynamic characteristics of a forward swept wing

Since the spanwise flow direction and the leading edge vortex flow direction of a forward swept wing are opposite to those of an aft swept wing, flow separation occurs at the inboard section near the leading edge of a forward wing first [2]. Consequently, this phenomenon affects the aerodynamics loading distribution on the wing surface. Fig. 2 shows typical pressure distribution at inboard and outboard sections of a forward swept wing. At a low angle of attack ($\alpha \leq 4°$), a relatively large suction peak occurs at the inboard section near the leading edge; the pressure gradient is also large behind the peak. Furthermore, the flow travelling distance in this reversed pressure area is rather long, and consequently, flow separation occurs quite easily. This explains why flow separation appears first at the inboard section for a forward swept wing. When $\alpha > 8°$, the suction peak near the leading edge disappears. As the angle of attack increases , the suction at the front is gradually reduced while it is increased at the rear, and levels off the chordwise pressure distribution. This indicates that the inboard flow of a forward swept wing basically is a separated flow at a high angle of attack; however, the low pressure region near the leading edge at yhe outboard can hold up to a higher angle of attack. This is because leading edge vortices are generated from the wing tip for a forward swept wing, and their

dimensions are small and thus do not affect the leading edge main stream at a middle angle of attack; consequently, a relatively large leading edge low pressure zone and peak are maintained. As the angle of attack increases, the swept angle of the vortex axis increases. Consequently, the afterward vortices induce a low pressure region on the wing surface. The leading edge swept angle of this particular forward swept wing is not large enough, the created leading edge vortices are not strong enough, and breakup occurs early. This results not only in reducing the vortex lift, but also in decreasing the suction peak near the leading edge and aggravates the flow separation near the leading edge at the inboard section.

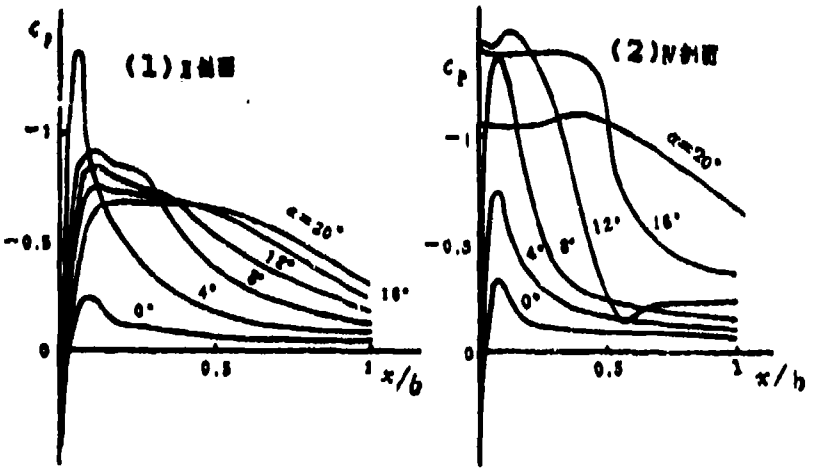

Fig. 2 Typical surface pressure distribution on cross-sections of a forward swept wing.
Key: (1) Cross-section II; (2) Cross-section IV.

Effects of the flow features stated above on aerodynamic forces are shown in Fig. 3. When the angle of attack is small, the lift-drag ratio of a forward swept wing is a bit larger than that of an aft swept wing. On the contrary, as the angle of attack

increases, the flow separation region at the inboard expands; thus the lift-drag ratio of a forward swept wing is smaller than that of an aft swept wing. Therefore, it is essential to find a means to slow down the flow separation which occurs at the inboard section of a forward swept wing.

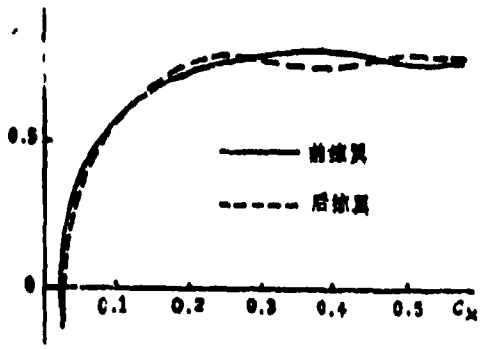

Fig. 3 Lift-drag characteristics for a wing-fuselage assembled body.
Key: (1) Forward swept wing; (2) Aft swept wing.

2. Improvement of inboard flow for a forward swept wing and Performance increasing

From the discussion above, we realize that the flowfield at the inboard section of a forward swept wing can be improved by increasing the kinematic energy inside the flow boundary layer or pushing the leading edge vortices forward.

a. Inboard strake: Installing strakes at the inboard section for a forward swept wing to control its flowfield can noticeably improve the lift-drag characteristics (for a high angle of attack). Under a mid or high angle of attack, the strength of strake vortices is large, and the nonlinear lifting vortices can improve the lift-drag ratio dramatically. However, the angle between the axis of strake vortex and the flow direction of the

leading edge vortex is quite large, and thus both flows block each other which limits the development of the vortices. Therefore, although strake vortices can improve the inboard flowfield, their efficacies can not be fully utilized.

b. Leading edge flap: The leading edge vortices of a forward swept wing are developed from its wing tips. The development of these leading edge vortices can be deferred by lowering the leading edge flap at the outer wing section, thus reducing their effects on the inboard flow, and consequently, improving the inboard flowfield. As shown in Fig. 4, a leading edge flap can increase the lift-drag ratio at a high angle of attack situation. However, under a higher angle of attack, separated vortices could possibly develope from its leading edge or even from its hinge line. Therefore, what shape is the best for a leading edge flap requires further studies.

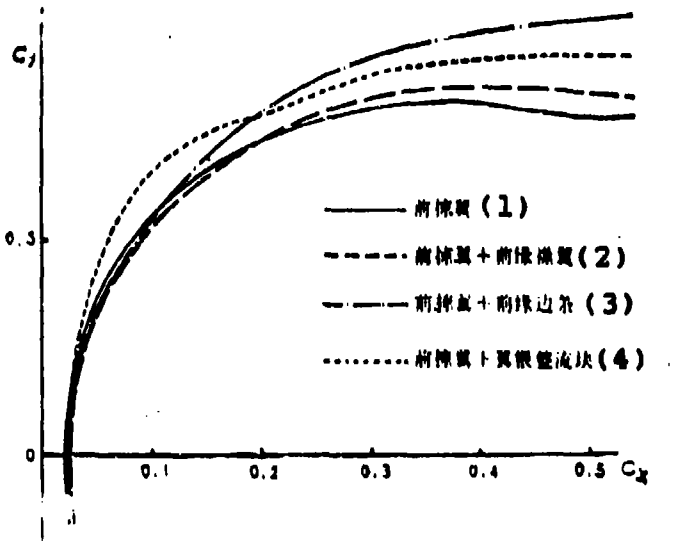

Fig. 4 Various means of improving lift-drag ratio.
Key: (1) Forward swept wing; (2) Forward swept wing plus a leading edge flap; (3) Forward swept wing plus leading edge strakes; (4) Forward swept wing plus a fairing.

c. Inboard fairing: Adding a swept backward fairing at the inboard section for a forward swept wing is to duplicate the inboard flow characteristics of an aft swept wing, thus improving the performance of a forward swept wing.

Figure 5 presents the pressure distributions at three inboard cross-sections of a forward swept wing after an inboard fairing is installed. The figure shows that the leading edge low pressure zone as well as the peak are recovered after an inboard fairing is added, especially at the two most inboard cross-sections. This can undoubtedly improve the lift-drag characteristic. Its lift-drag characteristic is shown in Fig. 4. Although its improvement at a high angle of attack is little less than a strake, the improvement is better under a mid angle of attack situation,

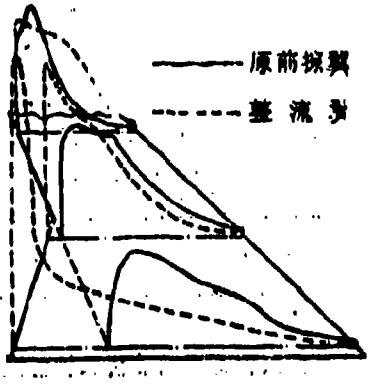

Fig. 5 Pressure distribution of a fairing. (α= 8°).
Key: (1) Original forward swept wing; (2) Fairing.

3. Aerodynamic characteristics of a canard configuration

The interference between the downwash flow and the vortex of a canard can defer the inboard flow separation for a forward swept wing or a forward swept wing with a fairing. The pressure distribution on the wing surface will also be changed. Fig. 6 shows that the canard decreases the lift at two inboard cross-sections; however, the leading edge low pressure zone and its peak are recovered. These changes not only make up for the partial lift loss, but also reduce the drag. Moreover, the lift at the outer wing section is noticeably increased. On the contrary, effects of a canard on an aft swept wing not only lose a larger lift, but also decrease the leading edge suction peak. Its lift improvement on outer wing section is also marginal. Consequently, this configuration of an aft swept wing could not only lose lif considerably, but also increase drag.

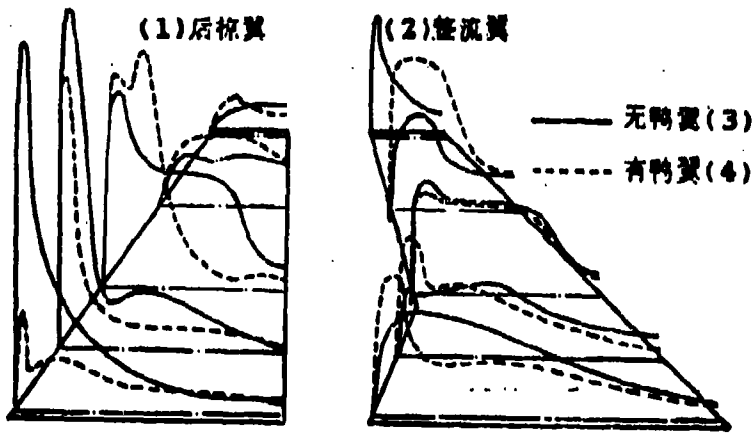

Fig. 6 Effect of a canard on pressure distribution (α = 12°)
Key: (1) Aft swept wing; (2) Fairing; (3) Without canard; (4) With canard.

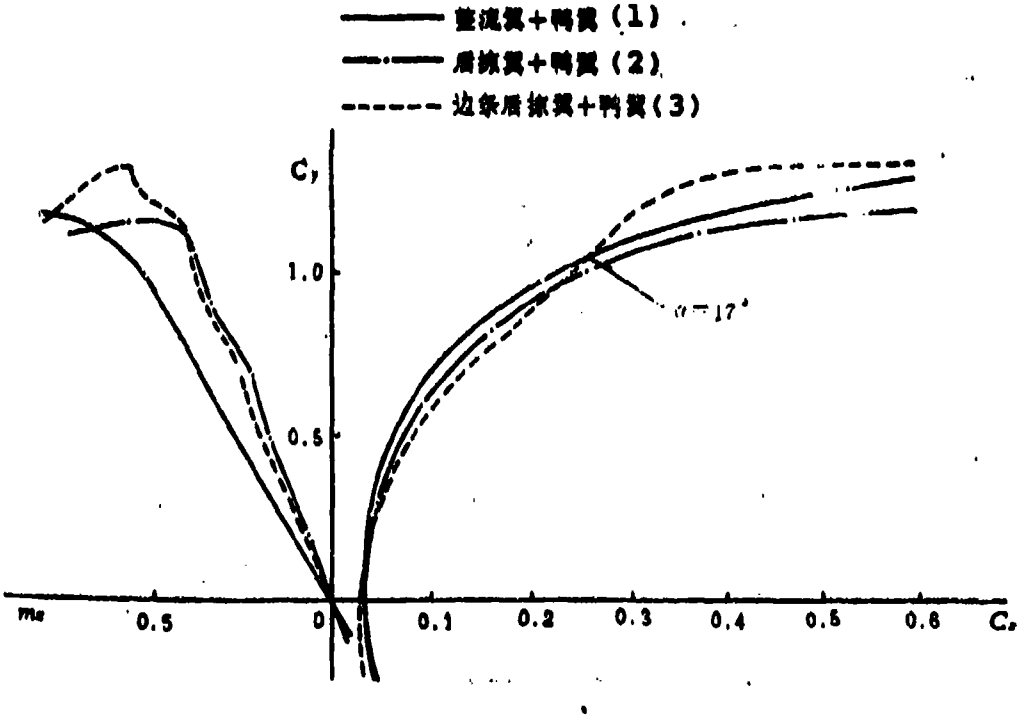

Fig. 7 Lift-drag characteristics and moment characteristics of a canard configuration.
Key: (1) Fairing plus canard; (2) Aft swept wing plus canard; (3) Aft swept wing with strake plus canard

Figure 7 shows the polarizing curves of canard configurations for three different types of wing. The canard configuration for a fairing is noticeably better than that for an aft swept wing in the entire range of angle of attack. This not only reflects the difference of two types of wing-fuselage combination, but also shows that the interference of a canard is favorable for a fairing. Comparing with an aft swept wing with strakes (both

lifting surface areas are equal), the lift-drag characteristic of a forward swept wing with a fairing is the best when $\alpha \leq 17°$ ($C_y \leq 1.05$). Under the same lift coefficient, the comparisons of drag reduction and lift-drag improvement are listed in Table 2.

In consequence of the improvement of the inboard flowfield for a forward swept wing with a fairing, the linearity of the pitching moment curve of a canard configuration is even better; however, its focus moves forward.

Table 2 Comparison of aerodynamic characteristics of a canard configuration for an aft swept wing with strake and a forward swept wing with a fairing.

C_y	0.3	0.4	0.5	0.6	0.7	0.8	0.9	1.0
(1)阻力降低	14.6%	16.7%	19.0%	18.1%	15.9%	13.9%	11%	3.5%
(2)升阻比提高	17%	20%	24%	22%	19%	16%	12%	4%

Key: (1) Drag reduction; (2) Lift-drag ratio improvement

IV. High Speed Aerodynamic Characteristics of a Forward Swept Wing

1. Aerodynamic characteristics of a forward swept wing

The varying trends of aerodynamic forces versus Ma for both forward swept and aft swept wings are similar.

a. Lift characteristics: In the subsonic range, C_y increases with Ma as shown in Fig. 8. Under the testing Mach number and forward swept angle range, all C_y^{α} values of the forward swept wing are less than that of the aft swept wing; however, the variation

amplitude of C_y^{α} versus Ma for the forward swept wing is smaller.

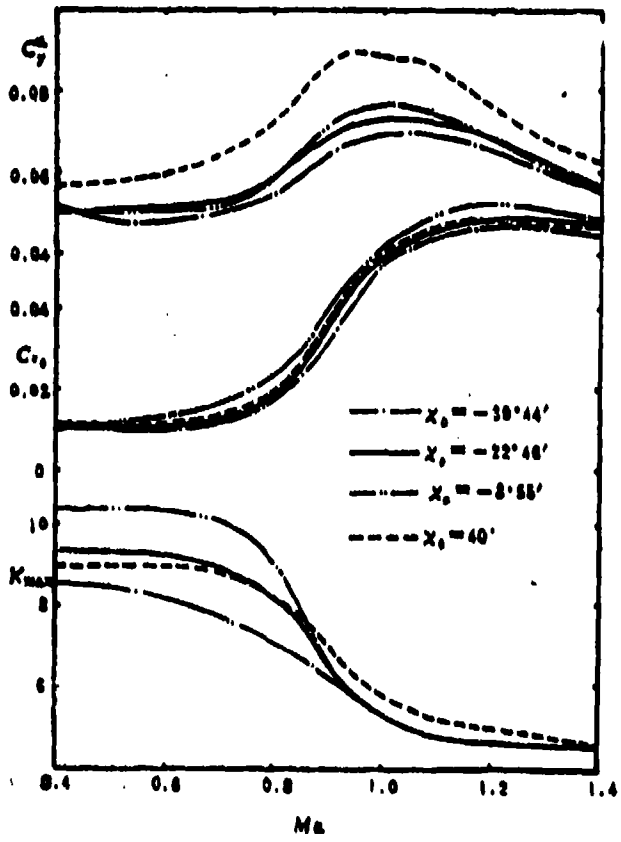

Fig. 8 High-speed characteristics of a forward swept wing.

b. Drag characteristics (Fig. 9): The varying trend of the zero lift drag coefficient, Cx_0 versus Ma is basically similar to that of an aft swept wing (Fig. 8). From the pressure distribution shown in Fig. 10, despite the fact that the increment is small, a sudden increase of pressure at the dashline on the forward swept wing surface indicates the existence of a shock wave which results in the sudden increase of Cx_0. When Ma = 1.1, Cx_0 reaches its maximum, and a bow shock is developed at this moment.

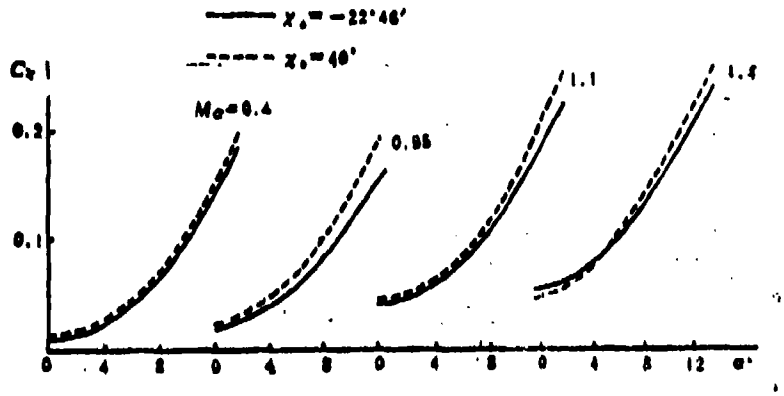

Fig. 9 Drag characteristics of a forward swept wing.

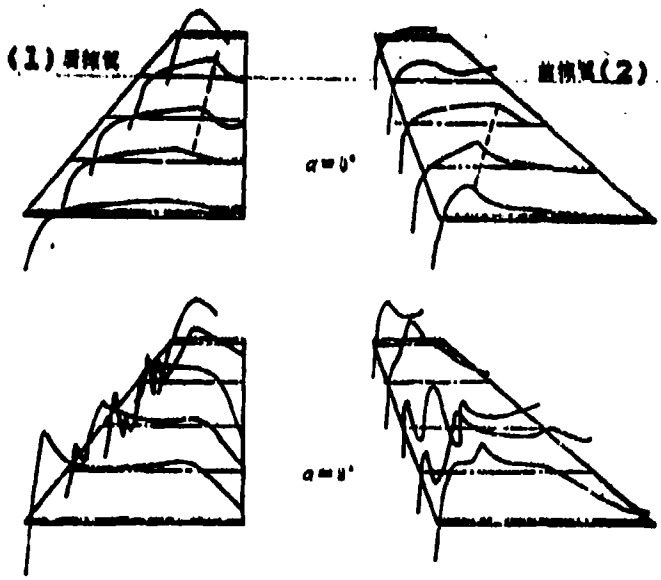

Fig. 10 High speed pressure distributions of a forward and an aft swept wings ($M_\infty = 0.85$)
Key: (1) Aft swept wing; (2) Forward swept wing.

From the pressure distribution of the $\alpha = 0°$ case (Fig. 10), the low pressure zone is close to the leading edge and its amplitude is large for a forward swept wing. Because the maximum thickness of

the airfoil is located at 35% of the chord, such a pressure distribution characteristic makes Cx_0 of a forward swept wing smaller than an aft swept wing. In supersonic regime, a bow shock appears in front of the leading edge, and also because the strength of the bow shock is related to the leading edge swept angle, therefore, Cx_0 of this testing forward swept wing is larger than that of the aft swept wing.

The airfoil model used in this experiment is symmetrical, when the angle of attack $\alpha = 0°$, Cy = 0 thus $Cx = Cx_0$. When $\alpha \neq 0°$, the wing generates lift as well as induced drag Cx_i (including lift-induced wave drag at high speed). The induced drag (generalized induced drag) can be written as:

$$C_{x_i} = C_x - C_{x_0} = \Delta C_x$$

where values of Cx_0 and Cx are obtained from experiments. The drag increment ΔCx thus can be calculated.

Table 3 Induced-drag coefficients which are induced by unit lift coefficients of forward, aft swept wings (α increases from 0° to 6°)

M₀ (1) 机翼		ΔC_x	ΔC_y	$\Delta C_x/\Delta C_y$
0.9	(2) 前掠翼	0.042	0.4	0.105
	(3) 后掠翼	0.049	0.47	0.104
1.1	(1) 前掠翼	0.049	0.44	0.111
	(2) 后掠翼	0.064	0.50	0.128
1.3	(1) 前掠翼	0.045	0.42	0.107
	(2) 后掠翼	0.054	0.48	0.113

Key: (1) Type of wing; (2) Forward swept wing; (3) Aft swept wing.

Table 3 shows that when Ma = 0.9, the drag coefficient increments which are induced by the unit lift coefficients of the forward swept and the aft swept wings are equivalent. However, when Ma = 1.1 and 1.2, the drag coefficient induced by the unit lift coefficient of the forward swept wing is larger than that by the aft swept wing. It is reduced by 12.5% at Ma = 1.1.

Figure 10 indicates that the low pressure zone near the leading edge of the aft swept wing suffers damage, thus suction near the leading edge at the middle of the span is smaller than that of the trailing section. This also indicates that strength of the shock at this location is larger. For the case of a forward swept wing, shock waves also appear at the same location, however, they are dispersed, and the suction near the leading edge is still larger than that at the trailing section. Consequently, the transonic induced drag of a forward swept wing is smaller.

The maximum lift-drag ratio, Kmax is shown in Fig. 8.

2. Improvement of high speed aerodynamic characteristic for a forward swept wing

a. Effects of leading and trailing edge swept angles

(1) Leading edge swept angle: Under unchanging conditions of the trailing edge swept angle, the aspect ratio as well as the total wing area, C_{y}^{α} decreases when the leading edge angle increases; Cx_0 can also decrease especially beyond the transonic

regime. For instance, when Ma = 1, Cx_0 of χ_0 = -39°44' is 0.002 smaller than that of χ = -8°55'; when Ma = 1.2, it is 0.006 smaller.

The maximum lift-drag ratio, Kmax, decreases as the leading edge swept angle increases in subsonic; however, the variation is small in supersonic.

(2) Trailing edge swept angle: Under unchanging conditions of the leading edge swept angle, the aspect ratio as well as the total wing area, C_y^{α} decreases when the trailing edge angle increases; Cx_0 also decreases as shown in Fig. 11.

Under unchanging conditions of the aspect ratio as well as the total wing area, increasing the trailing edge forward swept angle results in the increasing of the root-tip ratio, the wing area blocked by the fuselage increases, the wing area immersed in airflow decreases, thus reducing its friction drag. Beyond the transonic, increasing the trailing edge forward swept angle results in increasing the swept angle of the maximum thickness line, thus the swept angle of shock waves on the wing surface increases, the shock strength decreases, consequently, reducing the wave drag.

Although the drag of a large trailing edge forward swept angle is smaller, C_y^{α} is small, and therefore, the lift-drag ratio is small.

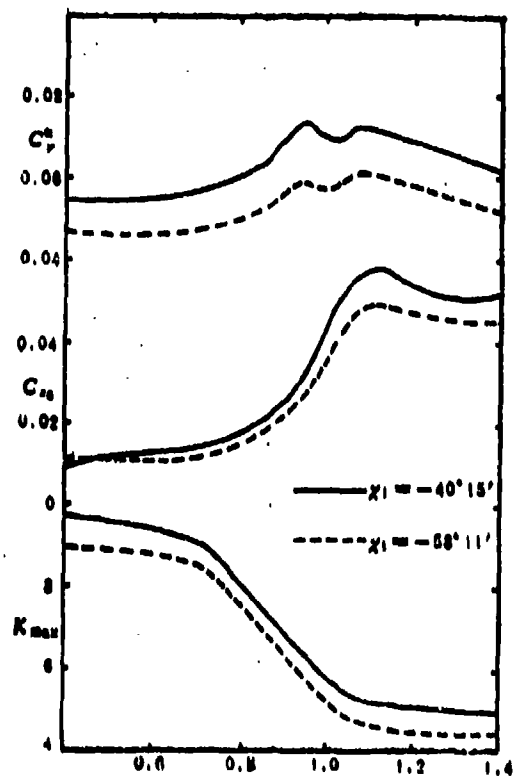

Fig. 11 Effects of trailing edge forward swept angle on the performance of forward swept wing.

b. Effect of inboard strake (Fig. 12)

Both C_y^α and C_{x_0} of a forward swept wing with strakes are larger than that of a forward swept wing without a strake. However, the maximum lift-drag ratio in transonic is smaller (in the range of a small angle of attack); this is consistent with results of the low speed case. Only when Ma > 0.9, Kmax of the former is then larger than the latter.

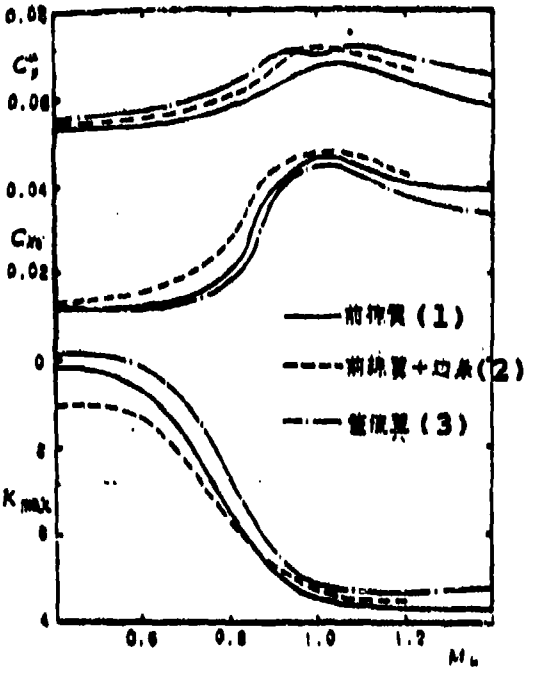

Fig. 12 Effects of strakes and fairings
Key: (1) Forward swept wing; (2) Forward swept wing plus strakes; (3) Wing with fairings.

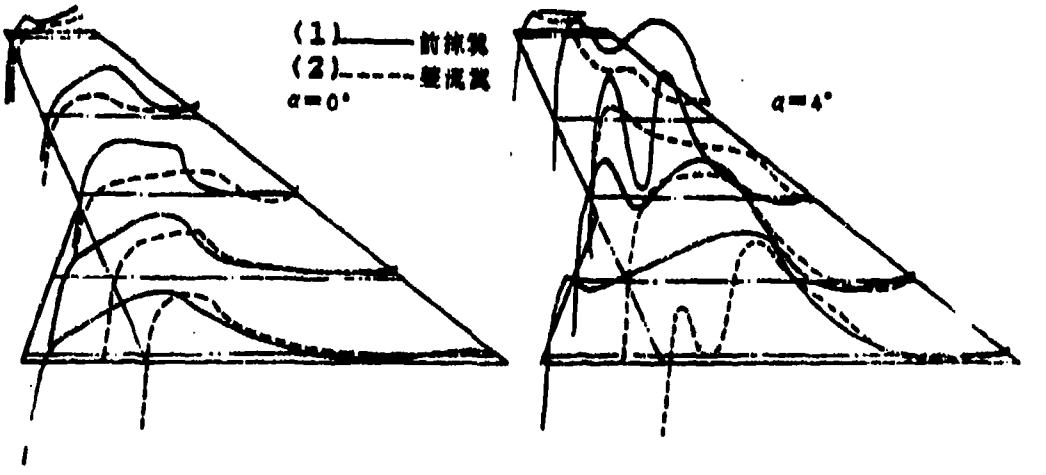

Fig. 13 Pressure distribution of a fairing wing, Ma=0.95
Key: (1) Forward swept wing; (2) Fairing wing.

c. Effect of inboard fairings

Figure 12 shows that effects of fairings are remarkable. From the pressure distribution on the fairing wing surface (Fig. 13), the fairing add additional loading at front parts of the first two inboard cross-sections (α= 0°), its resultant force location corresponds to that of a forward swept wing, and therefore, effect on the drag is small. However, the low pressure zone (as well as its amplitude) near the leading edge at outer cross-sections shows larger increments, consequently, reducing Cx_0 of the fairing wing. When α= 4°, besides of the additional loading because of the fairing, it also increases the loading at the original leading edge, thus increasing C_y^{α}.

3. Aerodynamic characteristics of a canard configuration

Figure 14 presents the characteristics of canard configurations for three different main wings, of which the values of both C_y^{α} and Kmax include the contributions from canards. Compared with Fig. 8, the canard configuration makes C_y^{α} increase for both a forward and an aft swept wing. It increases 0.009 ~ 0.018 for the forward swept wing while increasing around 005 for the aft swept wing. In addition, the maximum increment occurs when Ma > 1 for the forward swept wing with a canard configuration, which indicates that a forward swept wing with canard configuration can gain the most benefit in the transonic regime. For a fairing wing with

canard configuration whose C_y^{α} is 0.001 ~ 0.002 higher than a forward swept wing with canard configuration, and 0.005 ~ 0.12 higher than a fairing wing without a canard

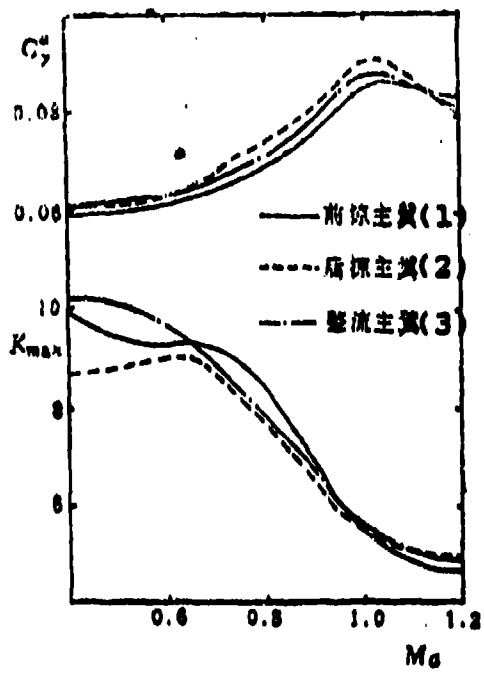

Fig. 14 Aerodynamic characteristic of canard configuration Key: (1) Forward swept wing; (2) Aft swept wing; (3) Fairing wing.

Figure 15 shows the effect of a canard on the pressure distribution of the main wing. When a canard exists, the pressure variation at the root section of a forward swept wing is small, and the suction peak near the leading edge at outer wing section increases. For an aft swept wing, the suction peak near the leading edge decreases over the entire wing. Although the loading increment at the trailing section can make up this loss, overall

drag increases. For a fairing wing, since its inboard section is sweptback and closes to the canard, therefore, it is strongly influenced by the canard, and consequently, the suction peak near the leading edge in this area increases which makes up the loss at the root section.

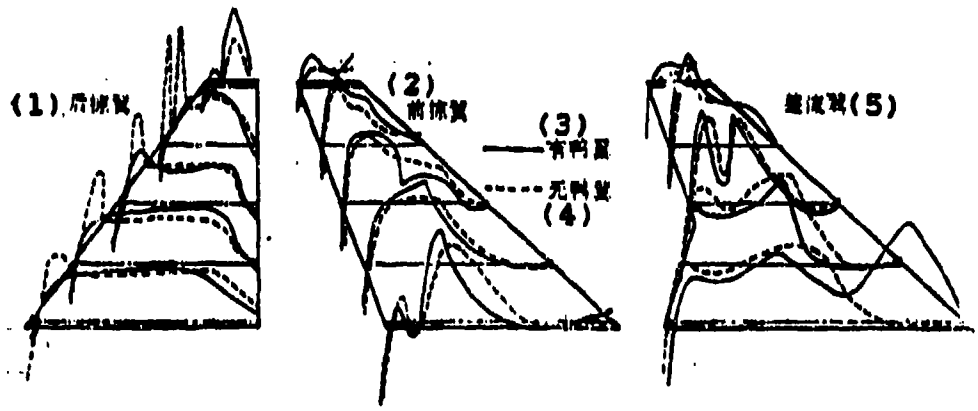

Fig. 15 Effect of canard on pressure distribution of a main wing (Ma = 0.95, α = 4°)
Key: (1) Aft swept wing; (2) Forward swept wing; (3) With canard; (4) Without canard; (5) Fairing wing.

V. Lift of Canard Under Main Wing Influence

Figure 16 shows the lift coefficient curves under the effects of different main wings. It clearly illustrates the difference of each main wing interference on the lift of the canard. The fairing wing is the best, the forward swept wing is next, and the aft swept wing is the worst.

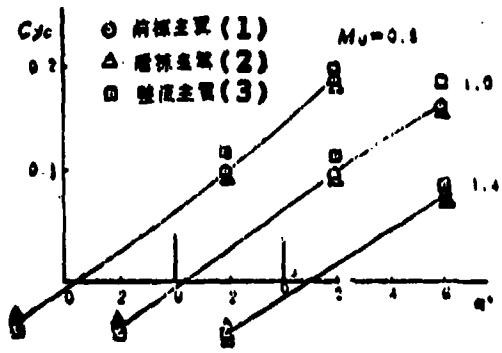

Fig. 16 Lift of canard under different main wing influence. Key: (1) Forward swept wing; (2) Aft swept wing; (3) Fairing wing.

VI. Conclusion

1. A forward swept wing possesses less drag, especial the high speed induced drag.

2. Under a small angle of attack, the lift-drag characteristic of a forward swept wing is good. At a higher angle of attack, the early flow separation occurring at the inboard section limits the improvement of a forward swept wing performance. This explains the importance of inboard flow improvement for a forward swept wing.

3. Adding a fairing at the inboard section is an effective way to improve the flowfield at the wing root which can increase the entire lift-drag ratio.

4. Adopting the canard configuration can create better interference effects for a forward swept wing than for an aft swept wing. It is even better for a fairing wing.

The authors appreciate the instructions and help provided by Prof. Lo Shijun, Qin Pizhao, Chen Inxue, and Fan Jichuan, etc.. Thanks are also due to Mr. Zhang Lizhuang for his participation of the work.

Literature:

[1] Robinson, M.R. and Robinson, D. A., Forward Swept Wing (FSW) Design: A High Payoff Through Technology Integration, AIAA paper 80-1884 (1980)

[2] Zhang Lizhuang, Wang Xuejian, Ko Yaobin and Zhang Binjiang, Study on Low Speed Aerodynamic for a Forward Swept Wing, China Aeronautical Technology HJB830138, (1983)

DISTRIBUTION LIST

DISTRIBUTION DIRECT TO RECIPIENT

ORGANIZATION	MICROFICHE
A205 DMAHTC	1
A210 DMAAC	1
B344 DIA/RTS-2C	9
C043 USAMIIA	1
C500 TRADOC	1
C1 BALLISTIC RES LAB	1
C510 R&T LABS/AVRADCOM	1
C513 ARRADCOM	1
C535 AVRADCOM/TSARCOM	1
C539 TRASANA	1
C591 FSTC	4
C619 MIA REDSTONE	1
D008 NISC	1
E053 HQ USAF/INET	1
E404 AEDC/DOF	1
E408 AFWL	1
E410 AD/IND	1
E429 SD/IND	1
P005 DOE/ISA/DDI	1
P050 CIA/OCR/ADD/SD	2
AFIT/LDE	1
FTD	1
CCN	1
NIA/PHS	1
LLNL/Code L-389	1
NASA/NST-44	1
NSA/T513/TDL	2
ASD/FTD/IQLA	1
FSL/NIX-3	1